CHAPTER 3

Quantitative Imaging of the Green Fluorescent Protein (GFP)

David W. Piston, George H. Patterson, and Susan M. Knobel

Department of Molecular Physiology and Biophysics
Vanderbilt University
Nashville, Tennessee 37232

I. Introduction
II. Factors That Influence/Limit Quantitation of GFP in Fluorescence Microscopy
    A. Fluorescence Properties of GFP That Are Important for Quantitative Imaging
    B. Quantitative Imaging of Fluorescence in a Microscope
    C. Microscopy Modes for Quantitative Fluorescence Imaging
III. Applications of LSCM for Quantitative Imaging of GFP
    A. Setting Up the Confocal Microscope
    B. Preparation and Imaging of Standards
    C. Time-Lapse Imaging
IV. Preparation of Purified GFP Samples
    A. Plasmid Construct
    B. Protein Expression and Purification
References

I. Introduction

The advent of GFP as an expression marker in heterologous systems stands as one of the most significant advances for optical microscopy of living cells (Chalfie *et al.*, 1994). A major advantage of GFP is that it opens up the possibility of many experiments that are not possible using other existing fluorescence techniques. Among these new applications are the use of GFP as a real-time reporter gene in living systems, a dynamic marker for subcellular structures and organelles, and a tracer of intracellular protein trafficking. However, another application of GFP that has not yet been fully developed is its use as a quantitative reporter of polypeptide concentrations and dynamics. For example, immunoflu-

METHODS IN CELL BIOLOGY, VOL. 58

0091-679X/99 $25.00

orescence intensity can be measured accurately, but the absolute values of the target molecule are always uncertain due to limitations of the immunoreaction chemistry. On the other hand, it is possible to couple a single GFP to each target polypeptide, thus overcoming the uncertainties in fluorophore/target ratio or nonspecificity of labeling. Although genetic manipulations have generated GFP molecules with nearly ideal properties for fluorescence microscopy, GFP is not a panacea, and its use brings up a new set of potential problems that may affect any quantitative imaging.

In this chapter, we will discuss the properties of GFP that are important for quantitative imaging. We will also discuss the properties of the fluorescence microscope that are important in quantitative imaging, such as microscope components (objective lenses, fluorescence filters, etc.), signal-to-noise ratio, detection linearity, and fluorophore saturation. Due to the large number of GFP mutants and the variety of potential biological applications, a comprehensive description of all possible quantitative imaging situations is not possible. Thus, most descriptions of methods for quantitative imaging will be limited to the use of fluorescein-like GFP mutants (e.g., ones containing the S65T mutation) with laser scanning confocal microscopy.

II. Factors That Influence/Limit Quantitation of GFP in Fluorescence Microscopy

A. Fluorescence Properties of GFP That Are Important for Quantitative Imaging

Spectral and physical properties of GFP affect the accuracy and usefulness of any quantitative measurement. Many of these properties, such as extinction coefficient, quantum yield, photobleaching rate, and pH dependence, can be measured with purified GFP *in vitro.* However, other important properties, especially the time course of chromophore formation and protein degradation *in vivo,* cannot be easily determined. In general one chooses the brightest, most photostable GFP available (Heim and Tsien, 1996; Cormack *et al.,* 1996), which may make complicated corrections for background and photobleaching unnecessary in less demanding applications. In addition, improving the performance of GFP by optimization of codon usage and using temperature stabilization mutations is still helpful in quantitative experiments (Siemering *et al.,* 1996; Patterson *et al.* 1997). For more demanding imaging applications in which the amount of GFP is low (i.e., in which GFP is fused to a protein that is in low abundance), the intrinsic properties of GFP will likely be the limiting factor. Therefore, it is necessary to understand the properties described here and use appropriate controls to minimize artifacts arising from them.

Photobleaching (photoinduced destruction of the chromophore) of GFP is much slower than fluorescein under similar conditions (Patterson *et al.,* 1997). This resistance to photobleaching is likely due to the protection of the GFP

chromophore by the tightly packed β-can structure (Ormo *et al.,* 1966; Yang *et al.,* 1996). Still, it is important to perform bleaching control experiments in any quantitative imaging experiment. Generally, one can simply acquire a time-lapse image series on GFP-labeled control cells (Niswender *et al.,* 1995) and measure the photobleaching time (photobleaching will generally give an exponential decay of intensity). This photobleaching time can then be used to correct the imaging experiments. If photobleaching becomes a limiting factor in the imaging of living cells, it is sometimes possible to reduce it by adding 10 μM Trolox (Rizzuto *et al.,* 1996). Using the S65T or F64L, S65T mutants of GFP, we find the photobleaching to be close to a single exponential decay with a half-time of >20 min for typical illumination intensities (Patterson *et al.,* 1997). However, it is very important to note that photobleaching of wild-type GFP is not characterized by a simple exponential decay. Wild-type GFP has two absorption peaks, 395 nm and 475 nm, which are related via an intramolecular rotation (isomerization) of the chromophore structure. The isomerization can be induced by irradiation of wild-type GFP with either 395- or 490-nm light, and the kinetics of this photoinduced reaction have recently been measured (Chattoraj *et al.,* 1996). Because both photoisomerization and photobleaching are occurring when wild-type GFP is irradiated at 488 nm, the temporal behavior is complicated: At first the photoisomerization dominates so the intensity increases, then, as the isomerization is complete and photobleaching begins to dominate, the intensity falls. Correcting a time-lapse series of images for such photoinduced behavior is difficult, so we have generally only used "red-shifted" fluorescein-like GFP mutants in our experiments.

Because the photobleaching of GFP is low, photodamage arising from GFP can also be expected to be low. Anecdotal evidence suggests that this is the case and indicates that GFP will be excellent for time-lapse and four-dimensional imaging. Although photodamage may be low, it is still important to perform viability controls during any imaging experiments on living cells. This is discussed in more detail in Section III.

The brightness of GFP and its mutants is also sensitive to pH. As an example, wild-type GFP shows relatively even brightness from pH 5 to pH 10 (Ward, 1981), whereas the S65T and F64L, S65T mutants are twofold brighter at pH 7 than at pH 6 (Patterson *et al.,* 1997). This behavior may affect any measurements in subcellular compartments such as lysosomes.

Finally, many physical parameters of GFP may dramatically affect its measurement but cannot be measured *in vitro.* The most important of these properties is the chromophore folding kinetics (or "turn-on" time). Because GFP chromophore formation requires oxidation and oxygen does not readily penetrate the GFP β-can structure, there can be a considerable delay (>1 h) between protein expression and the appearance of fluorescence. Unfortunately, it is not easy to distinguish between delays due to GFP expression (which one would like to measure) and those due to slow chromophore formation (which is an artifact of the GFP). In addition, the opposite process, GFP degradation, is also difficult

to determine *in vivo,* although evidence from many studies indicates that GFP is very stable in cells (see, e.g., Hampton *et al.,* 1996).

B. Quantitative Imaging of Fluorescence in a Microscope

The fluorescence microscope is commonly used for visualizing biological specimens. Its basic elements are the excitation light source, objective lens, filter cube, and detector. The choice of each of these components can affect the accuracy of any image quantitation. Generally, a mercury lamp or argon-ion laser is used for GFP excitation; these two sources have bright blue lines that are nearly ideal for GFPs containing the S65T mutation. For use with blue-shifted BFPs, other light sources, such as a xenon arc lamp, may be preferable. Regardless, the only issue for quantitative imaging is that there be enough excitation light available to obtain the required fluorescence signal. The second element is the objective lens, which is defined by three parameters: magnification, numerical aperture (NA), and lens design type. Despite general belief to the contrary, magnification is the least important of these parameters. It determines how large an object will appear in the eyepiece or detector, but not the resolution (i.e., the smallest detail that can be clearly observed) or brightness (the amount of fluorescence signal that will be collected). Both of these parameters are a function of the NA, which is the *most important* criterion for selection of an objective. The NA defines the amount of light that will enter the objective lens. The larger the NA, the higher the resolution and the brighter the GFP signal will be. In general, the highest NA lens available should be used, although the working distance (the maximum focal depth into the sample) decreases with higher NA. The lens design is also important, and for GFP a Fluor or Plan-Neofluor design is preferable because it will be brighter (i.e., it will pass more of the fluorescence signal) than a Plan-Apochromat design.

The two most critical components for quantitative imaging are the emission filter and the detector. The excitation filter, dichroic mirror, and emission filter are usually combined in a "filter cube." The choice of an excitation filter depends on the light source to be used for the fluorescence excitation. For example, with a mercury lamp an excitation filter with transmission of 450–490 nm is typically used. Similarly, the choice of dichroic mirror is defined by the excitation and emission filters, which leaves only the choice of the emission filter.

The general rule of thumb for GFP visualization is that if the level of GFP expression is high enough, GFP can be easily imaged (or even observed by eye) using a standard fluorescein filter set. However, use of a filter set designed specifically for GFP will enhance GFP signal collection (Niswender *et al.,* 1995; Endow and Komma, 1996). A dedicated filter set for quantitative imaging of GFP should use a narrow bandpass filter to maximize the collection of GFP signal versus the collection of background (usually due to autofluorescence). With a narrow bandpass filter, the sharp green GFP signal is preferentially passed to the detector over the greenish yellow or greenish orange background of cellular

autofluorescence (autofluorescence generally exhibits a very broad spectrum, whereas the GFP emission is relatively narrow). In principle, one would choose the narrowest bandpass filter to increase the discrimination of the GFP over other background signals. However, the optimal passband of the filter will be limited by the required signal-to-noise ratio (S/N), as discussed later. The optimal bandpass (i.e., the narrowest bandpass that allows a sufficient S/N) should be determined for each imaging situation, but we have had good luck using filters with ~30 nm bandpass (e.g., a 27-nm bandpass centered at 512 nm for wild-type GFP). It should be noted that for qualitative applications a wider bandpass filter will yield a "prettier" image. In addition, the specific filter chosen depends not only on the GFP signal strength, but also on the fluorescence spectrum of the particular GFP being used.

The use of a narrow bandpass is demonstrated in Fig. 1, which shows HeLa cells transfected with a glucokinase–GFP fusion plasmid (Niswender *et al.*, 1995). The autofluorescence background is considerably more pronounced using the longpass filter (panel A). If the level of GFP expression is high, then the choice of filter would make little difference (see the cells labeled "a" and "b"). However, for a cell that is expressing very low levels of GFP (see cell "c"), it is difficult to distinguish the GFP signal from autofluorescence with a longpass filter, although this cell clearly stands out with the narrow bandpass emission filter.

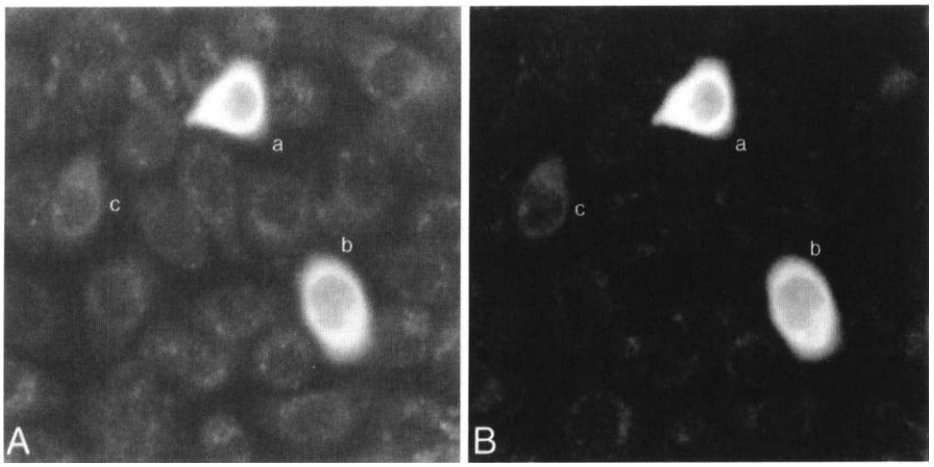

Fig. 1 Fluorescence images of HeLa cells transfected with a glucokinase–GFP fusion plasmid (Niswender *et al.*, 1995). Laser scanning confocal microscopy was performed using a Zeiss 410 microscope with a 40× Plan-Neofluar 1.3-NA oil-immersion objective. Excitation was by the 488-nm line of an argon–krypton-ion laser, and a Q498LP dichroic mirror was used. In panel A, a 515LP longpass emission filter was used, and in panel B a HQ512/27 emission filter designed specifically for GFP was used. Three GFP-positive cells (labeled a, b, c) can be seen in each panel.

The detectors that are typically used for quantitative microscopy are the photomultiplier tube (PMT) and the cooled charge-coupled device (CCD). PMTs are not imaging devices, so raster scanning (as is used in LSCM) must be performed to build up the image. Conversely, CCD cameras *are* imaging devices and can basically be used as a sensitive and linearly responding "eye." Other digital imaging cameras can be used for quantitative imaging as long as they yield a linear response to the fluorescence signals, but because film does not have a linear response, rigorous quantitation of photographs is not possible. One important design criterion for mounting the detector to the microscope is to avoid using an intermediate eyepiece lens. For example, an "iso C" mount connects the camera directly to the microscope with no extra lenses, which yields maximal optical efficiency. Although both PMT and CCD detectors have their own strengths and weaknesses, the usual bottom line is that PMTs are useful in microspectrofluorometry and laser scanning confocal microscopy (LSCM), whereas CCDs are more useful in widefield microscopy. Regardless of the detector used, basic principles such as the signal-to-noise ratio, detection linearity, and fluorophore saturation must be understood to ensure the accuracy of any quantitation.

The most important parameter for defining the usefulness of quantitative imaging is the signal-to-noise ratio (S/N). In modern commercial fluorescence microscopes the S/N is generally given by the shot noise, which is defined as the square root of the number of photons collected. Some systematic errors may be introduced in the detection system, but they are small compared to the shot noise for the two detectors, PMT and CCD camera, discussed in this chapter. For example, if one collects 100 photons per pixel the noise would be expected to be $\sqrt{100} = 10$, or 10% of the signal, and for 10,000 photons per pixel, $\sqrt{10{,}000} = 100$, or 1% of the signal. These examples reflect the typical signal levels in fluorescence microscopy, and errors introduced in the detection electronics are usually less than 1%. It would appear that one would always want to attain a maximal S/N, but in reality, factors such as photobleaching, fluorophore saturation, number of fluorophores in the sample, and spatial resolution limit the available S/N.

Photobleaching is often the ultimate limiting factor in fluorescence microscopy. Although the photobleaching rate of GFP is slow (as discussed earlier), photobleaching can still limit the amount of signal that can be obtained from a GFP-labeled sample. Another limiting factor, fluorophore saturation, does not occur in widefield fluorescence microscopy, but in LSCM, excitation intensities high enough to reach saturation are sometimes used. Saturation occurs when all the available fluorophores are constantly in the excited state, so that an increase in excitation light gives no increase in fluorescence. In this case, it is very difficult to calibrate fluorescence signals due to the introduced nonlinearity. Saturation can be avoided, though, by lowering the laser input power, and in general, the lowest excitation power that yields a sufficient S/N should be used. The number of fluorophores per pixel also limits the S/N. Each fluorophore can only generate

one fluorescence photon at a time, so to obtain a high S/N, a large number of fluorophores is required. In addition, if a high degree of spatial resolution is required, then there will be fewer fluorophores in each pixel, which will limit the S/N.

Another consideration in the detection system is its linearity and offset. Both PMT and CCD detectors are highly linear, but it is sometimes possible to adjust the offset (sometimes called black level). This should be set so that the image reads ~0 (in analog-to-digital units, ADU) when there is no fluorescence coming from the sample. If there is a nonzero offset in the system, then it will not be possible to quantitate accurately differences between images. For example, if there is an offset of 10 ADU, then a cell with an average value of 30 ADU would actually contain twice as much GFP as one with an average value of 20 ADU (30 − 10 = 20, which is twice 20 − 10 = 10). A negative offset causes even worse problems, because cells with the GFP signal may not even show up in the image. Details about how to set the correct offset in LSCM are given in Section III.

C. Microscopy Modes for Quantitative Fluorescence Imaging

Each technique that is used to measure fluorescence has advantages and limitations that require special consideration. Because many GFP mutants with altered spectral characteristics are now available, it is impossible to detail the optimal quantitative imaging criteria for each GFP mutant in every specimen with each type of instrument. The one basic principle that governs the visualization of GFP is to maximize the GFP signal over existing background. Because the background varies from specimen to specimen, optimization of the GFP signal over background can be accomplished by a combination of different means. These may include selecting an excitation wavelength that minimizes autofluorescence of the specimen, using a narrower bandpass emission filter, or using a GFP variant that is optimized for the specific organism under consideration. Specific considerations related to instrument selection and use are described in this section for four different types of microscopy: microspectrofluorometry, widefield (or conventional) fluorescence microscopy, confocal microscopy, and two-photon excitation microscopy.

1. Microspectrofluorometry

One of the simplest ways to measure total fluorescence from a cell population is with a spectrofluorometer. Although this technique is not imaging based, it is a very useful way to measure GFP spectra both *in vitro* and *in vivo,* quantitate GFP signals, and help calibrate results from quantitative imaging experiments. In a spectrofluorometer, fluorescence is measured directly from a solution (this could be a cell suspension, a whole cell extract, a purified GFP sample, etc.) placed in a cuvette, so very little special preparation is needed. For some mammalian cells

that are particularly adherent, a stir bar must be used in the cuvette, and most commercial spectrofluorometers have accessories for stirring the sample. In general, samples should be diluted to an optical density (O.D.) of less than 1.0. We typically measure fluorescence preparations in the spectrofluorometer at an O.D. of 0.1 or less. A useful variation of the spectrofluorometer is the microspectrofluorometer, in which the sample is observed on an attached microscope stage instead of in a cuvette. Although it still uses cell preparations (mounted on slides, perfusion chambers, etc.), this system give a couple of advantages over imaging methods. First, because many cells are usually observed in the field of view, the fluorescence signal is much larger than in an imaging experiment. This increases the S/N and also allows a lower excitation intensity, which in turn can reduce any possible photodamage to the cells. Second, one can acquire a complete fluorescence spectra. This can yield separation of many different GFP variants and may prove extremely useful for FRET experiments based on multiple GFPs. Of course, the microspectrofluorometer has the major disadvantage that there is no subcellular resolution.

2. Conventional Microscopy Using a Cooled CCD Camera

A conventional fluorescence microscope can be used for quantitative imaging by equipping it with a low-light, linear-response camera. These cameras are typically based on a CCD chip, which is inherently extremely linear and introduces little offset. Thermoelectric cooling of a CCD detector greatly improves sensitivity by reducing electronic noise, thus yielding essentially zero background, high dynamic range (16 bits = 2^{16} gray scales), and high detection efficiency (40 to 80%). Because low illumination levels can be used with this type of imaging detector, fluorophore saturation is not a problem. In addition, it is possible to use a long integration time so that very low light levels can be detected, but in living samples, usable integration times may be limited by the time scale of the biological events under investigation.

The use of a cooled CCD permits quantitation of GFP signals, especially in thin samples such as cell monolayers. However, because the CCD is used on a conventional fluorescence microscope, there is no discrimination between in-focus and out-of-focus fluorescence. Therefore, image quantitation can be complicated due to nonuniformities in cell thickness (i.e., a thicker cell can easily be confused for a cell with higher GFP expression). In some cases in which out-of-focus background is a problem, image deconvolution (described later) can be used to allow accurate quantitation and subcellular resolution.

In practice, many of the factors that must be considered for quantitative imaging with a CCD camera are the same as those for LSCM (see Section III), especially for time-lapse imaging. Some issues, though, are specific for use with a CCD. One requirement is a computerized image acquisition system that is capable of controlling the camera, shutter, and focus motor. Synchronization of the shutter and camera so that the samples are irradiated with excitation illumina-

tion only when the camera is taking an exposure minimizes photodamage and photobleaching. Because of time constraints due to the dynamics of the process under observation, it is often not possible to optimize exposure times with respect to the camera's dynamic range for imaging live specimens. In these cases, it is sometimes possible to increase the image acquisition rate by increasing the illumination intensity, but often the optimal exposure times for acquiring images of good to acceptable quality over the observation time should be determined empirically. Usually, it is possible to reduce the illumination so that cells can be observed on the microscope stage for at least an hour (Endow and Komma, 1996; Moores *et al.*, 1996).

a. Image Deconvolution

Because a widefield microscope collects fluorescence from throughout the sample and the cells are not always of a uniform thickness, the volume that is contributing to the observed signal is unknown. This uncertainty greatly complicates any absolute quantitation. For this reason, we use confocal microscopy for our quantitative imaging applications. However, image deconvolution can allow absolute quantitation of widefield microscopy data by using a mathematical algorithm to deblur a three-dimensional data set (Agard *et al.*, 1989; Carrington *et al.*, 1990; Holmes *et al.*, 1995). The advent of fast desktop computers has allowed deconvolution to be useful to a wide variety of laboratories for many applications. However, deconvolution algorithms may introduce artifacts in the data set and are less useful on densely fluorescent samples. A "densely" fluorescent sample is one where fluorescence arises from many places in the cell or sample (i.e., not just the DNA or a single organelle). For instance, cytoplasmic staining or microtubule staining of an embryo may look like a blur in a widefield microscope, whereas a confocal image may show sharp detail. There is a point, for any given number of collected photons, at which deconvolution techniques can no longer find the details in the blurry image and deconvolve them. This point, however, has never been strictly determined, and each research team using deconvolution usually establishes its own rule of thumb about which samples are appropriate.

To use image deconvolution, three criteria must be met. First, a computer-controlled fluorescence microscope with a high-quality cooled CCD camera and an accurate motorized focus control is required. Optical sections are generally taken throughout the sample at 0.1- to 0.5-μm intervals, and from 4 to 128 sections are used to perform the deconvolution. To achieve the best results, the acquired data set must be optimized for every sample in terms of spacing and number of sections. Second, a powerful computer must be available for the image processing: Requirements depend mainly on the number of sections in the data set, but Pentium-based computers with sufficient memory can be used to deconvolve most data sets in under an hour. Third, the PSF (point spread function) of the microscope–how the microscope images a single point of fluorescence–must be carefully measured using small ($<$0.2-μm) fluorescent latex beads. Some

new algorithms, however, do not require a priori knowledge of the PSF (Holmes *et al.*, 1995).

3. Confocal Microscopy

Although limitations on quantitative imaging with a cooled CCD camera can sometimes be overcome through image deconvolution, we have found that confocal microscopy offers significant advantages for fluorescence quantitation in tissues and optically thick samples. Because a well-defined optical section (typically $\sim 1\ \mu$m thick) is acquired in confocal microscopy, nonuniformities in cell thickness are not a major problem. However, during imaging of thick samples such as tissue slices, the fluorescence signal may decrease as the focal plane moves deeper into the sample, making it more difficult to interpret the quantitative amount of GFP in the cells.

In a laser scanning confocal microscope, the illumination is scanned in a raster pattern to form the image and a PMT detector is used. In most confocal microscopes, PMTs usually give lower dynamic range (8 bits = 2^8 gray scales) and detection efficiency (15 to 30%) than a cooled CCD. Although it would be desirable to increase the detection efficiency, the 8-bit dynamic range is usually not a problem because generally fewer than 255 photons/pixel/scan are collected. Still, the excellent linearity of the PMT response, background rejection properties, and availability of appropriate lasers (particularly the 488-nm line of an argon-ion laser) make confocal microscopy near ideal for quantitative imaging of GFP fluorescence. The use of confocal microscopy for quantitative imaging of the fluorescein-like S65T mutants of GFP is detailed in Section III.

4. Two-Photon Excitation Microscopy

Two-photon excitation microscopy (TPEM) is a new alternative to confocal microscopy. Use of this technique eliminates out-of-focus photodamage, avoids chromatic aberrations, and provides high-resolution three-dimensional measurements. Two-photon excitation arises from the simultaneous absorption of two photons, each of which is half the energy required for the transition to the excited electronic state of the fluorophore. In practice, two-photon excitation is made possible by the very high local instantaneous intensity that is provided by a combination of diffraction-limited focusing of a single laser beam in the microscope and the temporal concentration of a subpicosecond mode-locked laser. Resultant instantaneous peak excitation intensities are 10^6 times greater than those that are typical in confocal microscopy, but the pulse duty cycle of 10^{-5} maintains the average input power at less than 10 mW, which is only slightly greater than the power that is typically used in conventional confocal microscopy. Currently, the cost of state-of-the-art lasers, which are required for TPEM, has limited this technique to only a few laboratories. However, the field of ultrafast lasers is undergoing rapid development, and as the price of lasers decreases

over the next 10 years, TPEM may become a widely used method of optical sectioning microscopy.

Three properties of two-photon excitation provide the significant advantages over conventional optical sectioning microscopies for the study of UV excitable fluorophores in thick samples:

1. The excitation is limited to the focal volume due to the second-order dependence of the two-photon excitation on intensity and the decrease in intensity with the square of the distance from the focal plane. The excitation localization yields three-dimensional discrimination equivalent to an ideal confocal microscope without requiring a confocal spatial filter. Absence of the need to descan the fluorescence to pass a confocal aperture enhances fluorescence collection efficiency. Confinement of fluorophore excitation to the focal volume minimizes photobleaching and photodamage associated with UV illumination–the ultimate limiting factors in fluorescence microscopy of living cells and tissues.

2. Two-photon excitation allows imaging of UV fluorophores with conventional visible light optics in the scanning and detection systems because both the red excitation light (~700 nm) and the blue fluorescence (>400 nm) are within the visible spectrum.

3. Red light interacts much less strongly than UV light with most living cells and tissues (aside from plant cells) because fewer biological molecules absorb at longer wavelengths and red light is scattered less than shorter wavelengths. This nearly eliminates out-of-focus photodamage and background, and allows most of the input power to reach the focal plane. The relative transparency of biological specimens at 700 nm permits deeper sectioning than would be possible with UV excitation.

A limitation of TPEM is that the two-photon excitation spectrum may bear little resemblance to the one-photon absorption profile. GFP is easy to use in TPEM, however, because the two-photon excitation spectra of both wild-type GFP and the S65T mutant have been shown to overlap twice the one-photon absorption spectra, with the same relative absorption cross sections (Xu *et al.*, 1996). This overlap means that the major absorption peak of 395 nm for wild-type GFP is found at 2 × 395 nm (790 nm) with two-photon excitation. Preliminary results show a similar behavior for two-photon excitation of the F64L, S65T double mutant, and also that it is one of the strongest two-photon absorbers ever measured (C. Xu, M. Albolta, and W. W. Webb, personal communication). This is consistent with the extremely large one-photon absorption of this double mutant. Using wild-type GFP, useful two-photon-excited images have been obtained using ~790- (Niswender *et al.*, 1995; Patterson *et al.*, 1997) and ~900-nm (Potter *et al.*, 1996) excitation from a Ti:Sapphire laser.

The use of two-photon excitation microscopy is identical to that of confocal microscopy (as described later) except for the use of a different laser and elimination of the confocal pinhole. Currently, the laser of choice for TPEM is an

ultrafast mode-locked Ti:Sapphire (e.g., Coherent Mira or Spectra-Physics Tsunami) pumped by either an argon-ion laser or an all-solid-state, frequency-doubled Nd:YAG laser that has recently achieved the power levels necessary for this application. The mode-locked Ti:Sapphire laser produces ~100-fs pulses at a repetition rate of ~100 MHz and can be tuned over a broad range of output wavelengths from 700 to 1100 nm, allowing two-photon excitation of most UV and visibly excited fluorophores. The ability to adjust laser wavelength, though, makes this laser considerably more complicated than the "turnkey" lasers used in confocal microscopy.

In the future, ultrafast lasers yielding a single wavelength or a small group of selected wavelengths may allow the development of easy-to-use and relatively inexpensive two-photon excitation microscopes. Most current two-photon excitation systems have been built around a confocal laser scanning microscope, but because the pinhole is not needed to obtain optical sectioning, it should be opened fully or removed when using two-photon excitation. The lack of a pinhole requirement also allows for various other detection schemes. For instance, one can use a CCD camera or full-field photomultiplier detector to increase the fluorescence collection efficiency and still acquire optical sections from thick samples. The lasers and detection schemes available have been described in detail elsewhere (Denk *et al.*, 1995).

III. Applications of LSCM for Quantitative Imaging of GFP

The basic strategy used to quantitate GFP images is to perform parallel spectroscopy and microscopy experiments on a standard solution of fluorescein (Molecular Probes #F-1300, extinction coefficient = 90,000 cm^{-1} M^{-1} at 488-nm excitation, quantum yield = 85%) and a purified GFP solution, and compare these results to images of GFP-labeled cells. We have used both GST–GFP and His_6–GFP (Patterson *et al.*, 1997) for fast and easy GFP purification (a useful protocol for His_6–GFP purification is given in Section IV), and in neither case did we find any photophysical differences between purified GFP and the purified fusion proteins. Once a purified GFP sample is obtained, its concentration can be determined by absorption and fluorescence spectroscopy using the known extinction coefficient and quantum yield of the particular form of GFP being used (Heim and Tsien, 1996; Patterson *et al.*, 1997). For example, the S65T mutant of GFP has an extinction coefficient of ~55,000 cm^{-1} M^{-1} at 488 nm (Patterson *et al.*, 1997). The concentration of the GFP sample is then calculated from the absorption relative to fluorescein, that is, if the absorption at 488 nm of the S65T sample is the same as that of a 1 μM fluorescein sample, the S65T concentration is [S65T] = [fluorescein] (extinction coefficient of fluorescein/extinction coefficient of S65T) = 1 $\mu M \times (90/55)$ = 1.64 μM. It is also helpful to compare any spectral determination of GFP concentration with a standard biochemical method, such as the BCA assay (Patterson *et al.*, 1997).

As described in Section II, it is important to set the correct gain and offset for the detection system. To begin, set the gain so that the image of a typical GFP-labeled cell is not saturating (i.e., no pixel values = 255). Once the correct gain is set, it should not be changed during the calibration or imaging steps. Next, the microscope offset must be set so that zero pixel value corresponds to zero fluorescence signal. This can be done using the fluorescein sample as follows: Image four concentrations (in a ratio of 1:2:3:4) of fluorescein that each give a good signal but for which the maximum pixel value is <255 at the gain used for the GFP imaging. Determine the mean pixel value of each image using the histogram command, and plot the mean pixel value versus the concentration. The resulting plot should be a straight line, and the *y*-intercept will go through zero when the black level is correctly set. If the *y*-intercept is positive the offset should be reduced, and if the *y*-intercept is negative the offset should be increased. Image the GFP-labeled cell again. It may require several trials to achieve the optimum gain/offset combination for your sample. Dilute or concentrate the GFP sample to match the signal obtained in the cell GFP image, and determine the concentrations of GFP in the cell over the linear range of the image data (pixel values = 0–255). This procedure is somewhat difficult and time-consuming, but it only needs to be done one time. Once the correct offset is obtained, it should not change unless there is a modification/repair to the detection system of the microscope.

The known GFP sample can now be compared with GFP-labeled cells imaged by the confocal microscope. This is done by comparing the mean pixel values of the regions of interest in images of GFP with the mean pixel values from known GFP standards. The GFP standards are simply various concentrations of purified GFP sealed in deep-well slides or embedded in polyacrylamide. The unknown GFP concentration is determined from the linear equation generated by the mean pixel values of the standards. In addition to estimating absolute levels of target proteins, the standards also give experimenters two important advantages. First, the standards provide a way to normalize imaging experiments performed under different conditions, such as day-to-day fluctuations in excitation power or different optical alignments. Second, even though GFP photobleaches slowly, the standards allow compensation of photobleaching that may occur over the course of a lengthy experiment.

A. Setting Up the Confocal Microscope

Many of the details here depend on the particular microscope used. We usually use the Zeiss LSM410 confocal microscope for our quantitative GFP experiments, but all currently available confocal microscopes are integrated with comprehensive software packages that allow time-lapse and three-dimensional image acquisition. In addition, most of the processing needed for accurate quantitative imaging can be done with the resident confocal software or NIH Image, which is available free from the National Institutes of Health Web page (http://hrsb.info.-

nih.gov/nih-image/). For experiments on living cells, it is almost always necessary to have a temperature-controlled sample chamber. For work on an inverted scope, it is important to have a sufficiently large opening to allow access to high-NA objectives. In addition, if perifusion of different solutions is used, we have found it extremely advantageous to heat the perfusate to the temperature of the cell bath before it reaches the sample chamber. All the protocols described here are normally performed using a 40×/1.3-NA Plan-Neofluar oil-immersion objective. For this 40x objective, we use a pinhole value of 60, which maximizes the signal-to-noise ratio in the confocal microscope (Sandison *et al.*, 1995). We use the 488-nm line of the argon-ion laser with custom filters from Chroma Technology (Brattleboro, VT), a Q498LP dichroic mirror, and an HQ512/27 bandpass filter.

When working with a new preparation of cells in a case in which we are not sure of the GFP intensity, we begin with the following procedure. First, place the cells on the microscope stage and focus on the cells using transmitted light. The use of phase contrast or Nomarski DIC is often helpful in locating the cells. To minimize photobleaching and photodamage, fluorescence should not be used to initially focus the microscope. If a temperature-controlled stage is used, the cells should be allowed to equilibrate in the sample chamber for ~10 min. Next, it is usually helpful to quickly observe the cells by eye with conventional epifluorescence to assure that there is a sufficient GFP signal and to gauge how strong this signal is. Preliminary examination is also helpful to find positive cells in transient transfection experiments in which only a small percentage of them may contain GFP. Once an appropriate cell has been found, let the confocal imaging begin. It is a good idea to start the laser scanning with a low laser power and a high PMT gain. For example, we start with laser power = 10 (out of 100), and contrast = 325. Conveniently, the correct offset on our LSM410 is brightness = 9800 for all contrast values between 200 and 400. The exact offset value is likely to be different for each LSM410, though, and for some microscopes, the correct offset may change depending on the gain used. It should be noted that on the Zeiss system, the F9 key will automatically adjust the contrast and brightness to give a low-noise image, but this will not give appropriate values for quantitative measurements. While scanning, the laser power should be increased until an image of the cell is visible on the display. Once an image has been acquired, the laser power and gain can be adjusted to optimize the image S/N, but this procedure should be performed as quickly as possible to minimize photobleaching and photodamage. For example, with brighter samples a lower gain can be used. If the GFP sample is extremely dim, the pinhole can be opened further to allow more light to be collected, but this will reduce the spatial discrimination of the confocal microscope and thus decrease the accuracy of any quantitation.

B. Preparation and Imaging of Standards

For most applications of this technique, a range of concentrations that bracket the expected levels in the region of interest should be prepared. If the concentra-

tion of GFP and/or its fusion partner is completely unknown, a good starting range is ~200 nm to 10 μM. The GFP standards for the deep-well slides consist of ~100-μl GFP solutions containing 100 μg/ml BSA to minimize adherence of the GFP to the glass surfaces. These are loaded into the slide well, covered with coverslips, and sealed with hot paraffin. Images from the middle of the homogeneous solutions will give fluorescent signals and thus mean pixel values indicative of that GFP concentration. Although this method works well and provides excellent quantitation, it requires the inconvenience of replacing the sample slide, culture dish, chamber, and so on with the standard slide. An alternative method is to embed the GFP in a polyacrylamide slab, place the slab with the sample, and image both simultaneously. The GFP is mixed with acrylamide–bisacrylamide and diluted with GFP elution buffer (see Section IV) to the appropriate concentrations for each. One μl of 10% ammonium persulfate (APS) and 0.5 μl of *N,N,N′,N′*-tetramethylethylenediamine (TEMED) per 100 μl solution are added and mixed thoroughly. Ten microliters are placed on a microscope slide, covered by a coverslip to form a flat GFP–polyacrylamide slab, and allowed to polymerize over 5 to 10 min at room temperature. Once the slab has polymerized, the coverslip can be removed, the slab can be sliced with a razor blade, and the pieces placed with samples for imaging experiments. An example of this method is shown in Fig. 2 (see color plate). Panel (A) shows the fluorescence, panel (B) shows the DIC, and (C) shows the overlay of GFP–polyacrylamide imaged simultaneously with yeast, *Saccharomyces cerevisiae,* growing on 1% agarose supplemented with medium. In regions close to the GFP–polyacrylamide slab, the DIC images of the yeast are slightly distorted, but the fluorescence images are not hampered at all.

C. Time-Lapse Imaging

One major strength of GFP is that, because it is used with living cells, temporal dynamics can be observed and measured using time-lapse imaging. Methods for time-lapse imaging are described in detail in Chapters 10 and 12, but we will list some of the considerations for such experiments. First, one must make sure that the sample does not move too much during the time lapse. This is very sample dependent; for example work with *Caenorhabditis elegans* is often performed on anesthetized animals. The sample can also appear to "move" if there is any drift in the microscope focus. Problems of focus drift can be overcome by manually refocusing during the time lapse, acquiring a full three-dimensional data set at each time point, or using a feedback-controlled focusing stage (these can maintain focus position to nanometer precision). Second, it is important to know that the sample remains viable throughout the imaging process. With embryos and whole organisms, a morphological viability assay can be used. With yeast cells, for instance, it is possible to observe the cells by eye using transmitted light and to confirm that cell division is continuing. For quantitative imaging, the only additional consideration is a correction for photobleaching effects. As described earlier, most photobleaching exhibits an exponential decay profile. In

this case, it is straightforward to correct any quantitation by a simple normalization to the exponential decay curve. However, for long-time-lapse series of GFP-labeled cells, the absolute quantitation can be complicated by the fact that new GFP is being expressed throughout the experimental period.

IV. Preparation of Purified GFP Samples

To use many of the methods described here, a source of purified GFP is required. Because the addition of an affinity tag does not greatly perturb GFP fluorescence, purification of Histidine-tagged proteins from *E. coli* offers a quick and easily prepared source of highly purified GFPs. The protocol listed here is from an earlier study of GFP comparisons and should be easily adaptable for any GFP mutant (Patterson *et al.*, 1997).

A. Plasmid Construct

The 2.9-kb plasmid pRSET A (Invitrogen Corporation, Carlsbad, CA) was used for expression of Histidine-tagged protein. The cDNA of GFP was subcloned in frame with the hexa-Histidine tag sequence to produce an N-terminal His_6 fusion protein. GFP was prepared by PCR amplification using the N-terminal primer containing a *Bam*HI site and the C-terminal primer containing an *Eco*RI site and the TU#65 plasmid as template. The amplification product was gel purified, digested with the restriction endonucleases, *Bam*HI and *Eco*RI, and ligated into a similarly digested pRSET A to produce the GFP expression plasmid. The pRSET plasmid was transformed into the *Escherichia coli* strain BL21 pLysS for protein expression. In this system, high-level expression is driven by the T7 promoter in front of the His6-tagged proteins and the T7 RNA polymerase is provided by the host BL21 strain (Studier *et al.*, 1990). The pRSET and pLysS plasmids confer ampicillin and chloramphenicol resistance, respectively, to the expression strain.

B. Protein Expression and Purification

The His-tagged GFP protein was expressed in *E. coli* grown at 28°C. A 100-ml starter culture grown overnight in Terrific Broth (Sambrook *et al.*, 1989) containing 100 μg/ml ampicillin and 25 μg/ml chloramphenicol at 37°C was used to inoculate a 1-liter culture at 28°C. This culture was incubated for 2 h, induced with 0.1 m*M* isopropylthio-β-D-galactopyranoside (IPTG), and grown for 5 h before harvesting by centrifugation. The cells were resuspended in sonication buffer (50 m*M* Na_2HPO_4, 300 m*M* NaCl, pH 8.0) and stored at −70°C until purification was continued. After thawing, the cells were lysed by incubation with lysozyme followed by sonication. Insoluble debris were pelleted by centrifugation. The supernatant was incubated with Ni NTA agarose (Qiagen

Inc., Chatsworth, CA) in a 15-ml conical tube (Sarstedt, Newton, NC) for 1 h at room temperature on a rocker platform. The resin was pelleted by slow centrifugation, the supernatant was removed, and the resin was washed once with sonication buffer containing 10 m*M* imidazole. The wash was repeated once with sonication buffer containing 50 m*M* imidazole. The resin was packed into columns and the proteins were eluted from the Ni NTA column with 1 ml of elution buffer (50 m*M* Na_2HPO_4, 300 m*M* NaCl, 200 m*M* imidazole, pH 8.0). Protein concentration was determined by BCA assay, and the purification efficiency was determined by scanning densitometry of SDS gels stained with Coomassie brilliant blue. Only proteins that are purified to >95% homogeneity should be used for standards.

References

Agard, D. A., Hiraoka, Y., Shaw, P., and Sedat, J. W. (1989). Fluorescence microscopy in three dimensions. *Methods Cell Biol.* **30,** 353–377.

Carrington, W. A., Fogarty, K. E., and Fay, F. S. (1990). 3D fluorescence imaging of single cells using image restoration. *In* "Non-invasive Techniques in Cell Biology" (Foskett, J. K., and Grinstein, S., Eds.) pp. 53–72. Wiley-Liss. New York.

Chalfie, M., Tu, Y., Euskirchen, G., Ward, W. W., and Prasher, D. C. (1994). Green fluorescent protein as a marker for gene expression. *Science* **263,** 802–805.

Chattoraj, M., King, B. A., Bublitz, G. U., and Boxer, S. G. (1996). Ultra-fast excited state dynamics in green fluorescent protein: multiple states and proton transfer. *Proc. Natl Acad. Sci. U. S. A.* **93,** 8362–8367.

Cormack, B. P., Valdivia, R. H., and Falkow, S. (1996). FACS-optimized mutants of the green fluorescent protein (GFP). *Gene* **173,** 33–38.

Denk, W., Piston, D. W., and Webb, W. W. (1995). Two-photon excitation in laser scanning microscopy. *In* "The Handbook of Biological Confocal Microscopy" (Pawley, J., Ed.) pp. 445–458. Plenum Press, New York.

Endow, S. A., and Komma, D. J. (1996). Centrosome and spindle function of the *Drosophila* Ncd microtubule motor visualized in live embryos using Ncd-GFP fusion proteins. *J. Cell Sci.* **109,** 2429–2442.

Hampton, R. Y., Koning, A., Wright, R., and Rine, J. (1996). *In vivo* examination of membrane protein localization and degradation with green fluorescent protein. *Proc. Natl. Acad. Sci. U. S. A.* **93,** 828–833.

Heim, R., and Tsien, R. Y. (1996). Engineering green fluorescent protein for improved brightness, longer wavelengths and fluorescence resonance energy transfer. *Curr. Biol.* **6,** 178–182.

Holmes, T. J., Bhattacharyya, S., Cooper, J. A., Hanzel, D., Krishnamurthi, V., Lin, W., Roysam, B., Szarowski, D. H., and Turner, J. N. (1995). Light microscopic images reconstructed by maximum likelihood deconvolution. *In* "The Handbook of Biological Confocal Microscopy" (Pawley, J., Ed.) pp. 389–402. Plenum Press, New York.

Moores, S. L., Sabry, J. H., and Spudich, J. A. (1996). Myosin dynamics in live *Dictyostelium* cells. *Proc. Natl Acad. Sci. U. S. A.* **93,** 443–446.

Niswender, K. D., Blackman, S. M., Rohde, L., Magnuson, M. A., and Piston, D. W. (1995). Quantitative imaging of green fluorescent protein in cultured cells: comparison of microscopic techniques, use in fusion proteins and detection limits. *J. Microscopy* **180,** 109–116.

Ormo, M., Cubitt, A. B., Kallio, K., Gross, L. A., Tsien, R. Y., and Remington, S. J. (1996). Crystal structure of the *Aequorea victoria* green fluorescent protein. *Science* **273,** 1392–1395.

Patterson, G. H., Knobel, S. M., Sharif, W. D., Kain, S. R., and Piston, D. W. (1997). Use of the Green Fluorescent Protein (GFP) and its mutants in quantitative fluorescence microscopy. *Biophys. J.* **73,** 2782–2790.

Potter, S. M., Wang, C.-M., Garrity, P. A., and Fraser, S. E. (1996). Intravital imaging of green fluorescent protein using two-photon laser-scanning microscopy. *Gene* **173,** 25–31.

Rizzuto, R., Brini, M., De Giorgi, F., Rossi, R., Heim, R., Tsien, R. Y., and Pozzan, T. (1996). Double labelling of subcellular structures with organelle-targeted GFP mutants *in vivo*. *Curr. Biol.* **6,** 183–188.

Sambrook, J., Fritsch, E. F., and T. Maniatis. (1989). Appendix A: Bacterial media, antibiotics, and bacterial strains. *In* "Molecular cloning: a laboratory manual" (C. Nolan, Ed.) p. A. 2. Cold Spring Harbor Laboratory Press, Plainview, NY.

Sandison, D. R., Piston, D. W., Williams, R. M., and Webb, W. W. (1995). Resolution, background rejection, and signal-to-noise in widefield and confocal microscopy. *Appl. Optics* **34,** 3576–3588.

Siemering, K. R., Golbik, R., Sever, R., and Haseloff, J. (1996). Mutations that suppress the thermosensitivity of green fluorescent protein. *Curr. Biol.* **6,** 1653–1663.

Studier, F. W., Rosenberg, A. H., Dunn, J. J., and Dubendorff, J. W. (1990). Use of T7 RNA polymerase to direct expression of cloned genes. *In* "Methods of Enzymology" (D. V. Goeddel, Ed.), Vol. 185, pp. 60–89. Academic Press, San Diego.

Ward, W. W. (1981). Properties of coelenterate green fluorescent proteins. *In* "Bioluminescence and Chemiluminescence" (DeLuca, M. A., and McElroy, W. D., Eds.) pp. 225–234. Academic Press, San Diego.

Xu, C., Zipfel, W., Shear, J. B., Williams, R. M., and Webb, W. W. (1996). Multiphoton fluorescence excitation: new spectral windows for biological nonlinear microscopy. *Proc. Natl. Acad. Sci. U. S. A.* **93,** 10763–10768.

Yang, F., Moss, L. G., and Phillips, G. N., Jr. (1996). The molecular structure of green fluorescent protein. *Nat. BioTech.* **14,** 1246–1251.